

Shape Memory Hooks Employed in Fasteners

D. Vokoun, D. Majtás, M. Frost, P. Sedlák, and P. Šittner

(Submitted October 17, 2008; in revised form December 9, 2008)

We study shape memory hooks employed in releasable fasteners. The designed fastener in question consists of two identical parts, each one containing an array of hooks made of the shape memory alloy with the pseudoelastic behavior at room temperature. The fastening function consists in interlocking of the hooks of the either part together. The firmness of the connection is tested for various hook geometry and heat treatment of the hooks. A model for the mechanical response of a loaded single shape memory hook is developed and described. Both the model and the experimental data indicate the firmness of the connection increases with increasing hook curvature and hook density. In the study, we also present the fastener manufacture using NiTi wires with a diameter of 150 μm .

Keywords fastener, modeling, NiTi hooks, pseudoelasticity

1. Introduction

Shape memory hooks may be used as fasteners (Fig. 1). In the recent shape memory alloy (SMA) fastener development, Powell et al. (Ref 1) construct an array of SMA hooks while each hook consists of either two kinds of SMAs or a SMA and other shape memory material. The hooks can open on an external stimulus (e.g., heating by electrical current) due to the shape memory effect. The main function of such a fastener is to interconnect the hook array with an array of loops and allow a release of the connection by making the hooks straight upon heating.

In our research, we study releasable fasteners made of SMA hooks utilizing the pseudoelastic effect. Although the pseudoelastic behavior of SMAs has been studied in numerous papers related to the SMAs, there is not much known about the mechanical behavior of pseudoelastic hooks made of NiTi alloys employed in SMA fasteners. The reason is first our application of the pseudoelastic effect is very specific and second, during the fastener releasing by pulling apart of the two hook arrays each individual hook is bent, especially in the curved part causing a complicated nonhomogeneous stress state. Additionally, not each hook is interlocked and the interlocked hooks are not being released at the same moment due to a certain variation in the hook length. Hence, the prediction of the thermo-mechanical behavior based on

geometrical and material parameters and SMA hook density is not easy.

If the substrates in Fig. 1 are flexible, our SMA fasteners may serve as a kind of Velcro fasteners. In the Velcro type fastener, the peel-off force is considerably smaller than the pulling force in the normal direction or in any other direction. In our study, we focus on the measurement of the normal pulling force. Therefore, the substrates for attaching SMA hook arrays in our study are rigid. However, flexible substrates may be used in our further study to employ the SMA hooks in the Velcro type fasteners. One may ask what is the advantage of the SMA hooks used as Velcro type fasteners if much cheaper plastic hooks can do the same job. Actually, the advantage is less noise during the hook release when compared to the release action of the typical Velcro fasteners. Furthermore, other advantages are better durability, heat resistance, or functioning in chemically aggressive environments. The noise reduction of SMA hooks is due to damping capacities of SMAs due to ongoing face change transformations.

In the first part of our study, we describe the SMA hook shape setting. Further, we deal with mechanical loading of a single NiTi hook providing with some experimental data. We measure the minimum force necessary for a separation of two interlocked hooks, one of which is NiTi hook and the other is a steel rigid hook. In this kind of measurement, we vary the hook curvature and the NiTi hook heat treatment. In the second part of the work, we introduce a simple 1D model capable of simulating the load-stroke curves during the unhooking process. Finally, in the third part, we introduce the hook array manufacture and some measurements with complete hook arrays where an attention is paid to the hook density while the overall unhooking force in the perpendicular direction is measured.

2. SMA Hook Shape Setting

A cold-drawn NiTi wire with a diameter of 0.5 mm purchased from a commercial company was shape-set with a special fixture (Fig. 2) causing the wire to have the shape of a hook after releasing from the fixture. The fixing device was

This article is an invited paper selected from presentations at Shape Memory and Superelastic Technologies 2008, held September 21–25, 2008, in Stresa, Italy, and has been expanded from the original presentation.

D. Vokoun, D. Majtás, M. Frost, and P. Šittner, Institute of Physics ASCR, v.v.i., Na Slovance 2, 182 00 Prague 8, Czech Republic; and **M. Frost and P. Sedlák**, Institute of Thermomechanics ASCR, v.v.i., Dolejškova 1402/5, 182 00 Prague 8, Czech Republic. Contact e-mail: vokoun@fzu.cz.

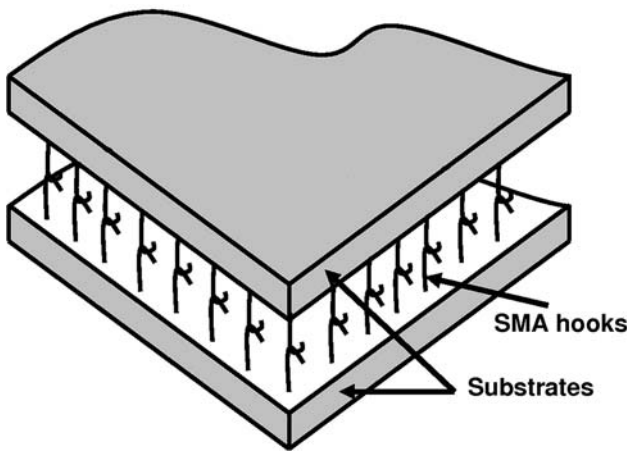


Fig. 1 A scheme of a SMA hook fastener

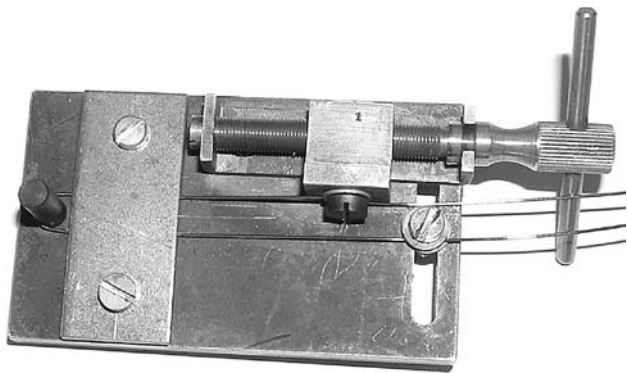


Fig. 2 A fixture for shape setting of the SMA hooks

designed to vary the NiTi wire hook curvature and to keep the hook prestressed. The shape-setting temperatures were 350 and 450 °C applied to the wire in the shape of a hook for 30 min.

We also prepared smaller SMA hooks using another cold-drawn NiTi wire with a diameter of 0.15 mm. The SMA hook shape setting was different: The wire was wound around a rectangular plate with a thickness of 0.8 mm and annealed at 350 °C for 30 min. The individual hooks were then cut from the shape-set superelastic wire.

Both the wires (diameters 0.15 and 0.5 mm) after the chosen heat treatment were superelastic at room temperatures. While the large hooks were used for single hook loading experiments and modeling, the smaller hooks were further manufactured into SMA hook arrays.

3. SMA Hook Loading Experiments

The single hook loading experiments were carried out with six various hook samples. The samples are listed in Table 1. The experimental setup is shown in Fig. 3. The long axes of both the hooks are co-linear. The hooks were pulled apart along the axis line while measuring the pulling force. We stopped pulling as soon as the unhooking happened. The unhooking event is characterized by a sharp drop of the measured force to the zero value.

The measured load-stroke curves in Fig. 4 can be grouped into three curve couples. Each curve couple corresponds to one of

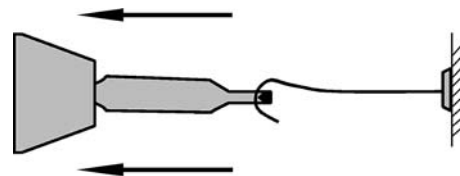


Fig. 3 A scheme of loading of a single SMA hook

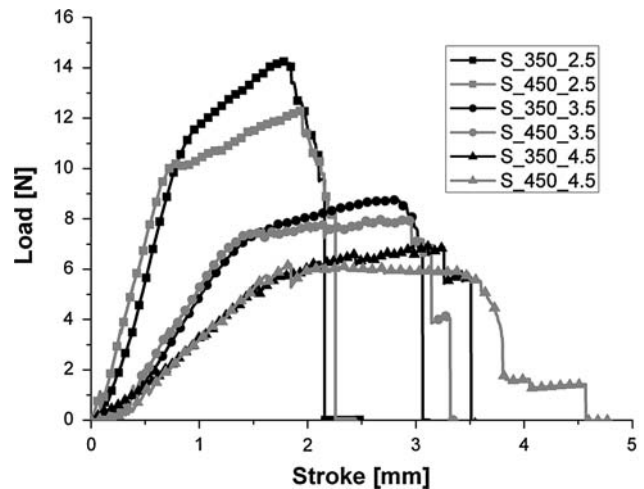


Fig. 4 The diagram of hook load vs. stroke for various samples

Table 1 A list of tested single SMA hook specimens

Sample	Heat treatment, °C	Hook inner diameter at the bent place, mm
S_350_2.5	350	2.5
S_450_2.5	450	2.5
S_350_3.5	350	3.5
S_450_3.5	450	3.5
S_350_4.5	350	4.5
S_450_4.5	450	4.5

the hook curvature. It means that the curves in one couple contain the data related to both the heat treatments. We can see that the curve course and the maximum force reached strongly depend on the hook curvature. The larger the curvature the larger maximum the force is. In each couple, the maximum force associated with the 350 °C heat treatment is higher than that associated with the 450 °C heat treatment. The reason for that can be seen in Fig. 5: The tensile stress-strain curve for the 350 °C heat treatment has higher upper transformational plateau than that one for the 450 °C heat treatment. Most of the curves in Fig. 4 have a rugged course due to the frictional force acting at the point of the contact between the two hooks (steel and SMA hook). It is worth noting that sample S_350_2.5 after unhooking did not return to its original shape due to caused plastic deformation.

4. Model

The main motivation for creating a mechanical model simulating the SMA hook loading as described in the previous part was the need to determine the minimum force necessary

for SMA hook releasing. However, the created model is additionally able to predict the whole load-stroke curves shown in Fig. 4 and load-stroke curves for SMA hooks of any other geometrical or material parameters.

For simulation of the material behavior, we used a pseudoelasticity module of the phenomenological 1D model iRLOOP (Ref 2). This module of the iRLOOP model, which was developed at IT and IP ASCR, v.v.i., in 2007 has the following features:

- keeps the concept of thermodynamic force linking stress and temperature, which drives the transformation processes,
- reliably describes both entire and partial martensite to austenite and reverse transformation processes with partial cycles and internal subloops,
- captures asymmetric behavior in tension and compression in pseudoelasticity,
- is able to be driven by prescribed evolution of strain and temperature of a wire, and
- is able to adapt to particular material by changing several experimentally well-measurable input parameters.

The model introduces two internal state variables: tensile martensite volume fraction, ξ^+ , and compressive martensite

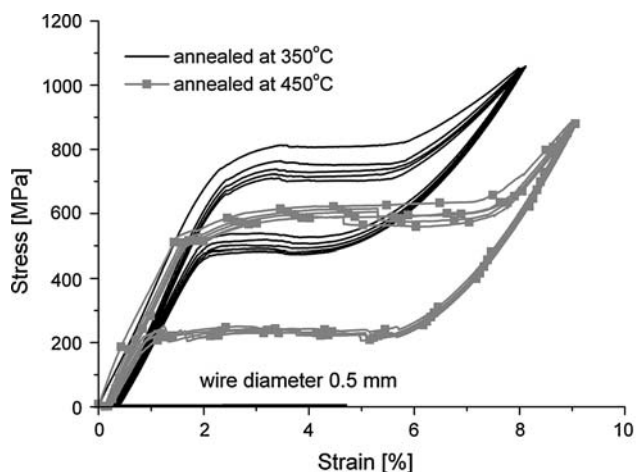


Fig. 5 The diagram of the tensile stress vs. strain dependence measured for the straight NiTi wire samples having the identical heat treatment as the SMA hooks

volume fraction, ξ^- . The value of tensile resp. compressive martensite depends on the driving force for martensitic transformation, ϕ^+ resp. ϕ^- defined as:

$$\begin{aligned} \phi^+ &= \frac{\sigma}{s^+} - (T - A_f) & s^+ &= \frac{c}{\Lambda^+} \\ \phi^- &= \frac{\sigma}{s^-} - (T - A_f) & s^- &= \frac{c}{\Lambda^-} \end{aligned} \quad (\text{Eq 1})$$

It also depends on the set of ordered pairs of real numbers called return points. In (1), Λ^+ and Λ^- are the transformation strains in tension and compression, and c is the material parameter. The model uses the adaptation of the Duhem-Madelung model of hysteresis described in Ref 3; the envelope functions of the hysteretic loop are approximated by piecewise linear functions which best fit the experimental data.

Since tensile and compressive martensite never appear simultaneously for temperature $T > A_f$ (austenite finish), which is the case of our study, we can consider the evolution of ξ^+ and ξ^- as completely independent and the constitutive equation for the total strain of the material in the simple form (thermal expansion neglected):

$$\varepsilon = (1 - (\xi^+ + \xi^-)) \frac{\sigma}{E_A} + (\xi^+ + \xi^-) \frac{\sigma}{E_M} + \Lambda^+ \xi^+ + \Lambda^- \xi^-, \quad (\text{Eq 2})$$

where E_M and E_A denote the Young modulus of martensite and austenite.

In the simulation of the SMA hook loading, the hook was divided to a system of beam elements, each of them consisting of several material slices-truss elements (Fig. 6). We assume

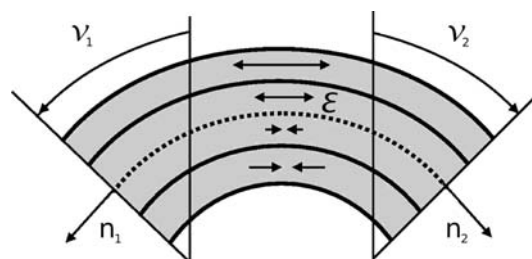


Fig. 6 The beam element consisting of several material slices-truss elements. The normal of cross section of the beam is assumed to be parallel to the beam axis

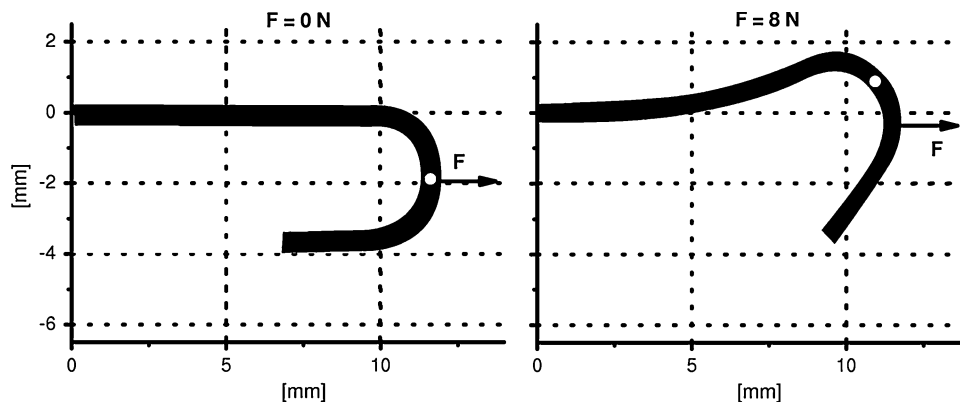
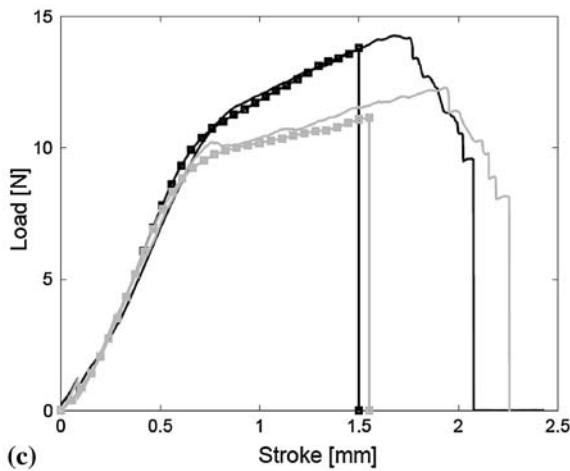
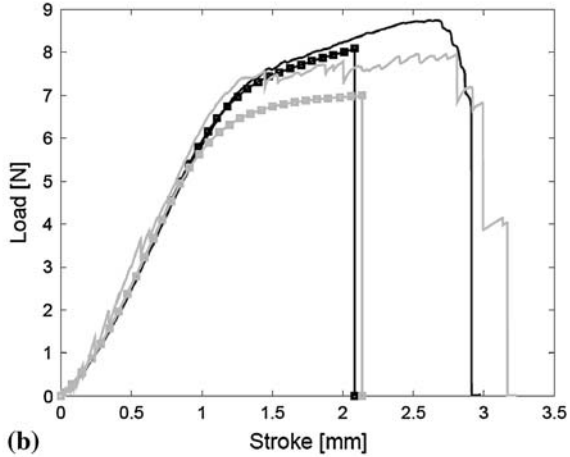
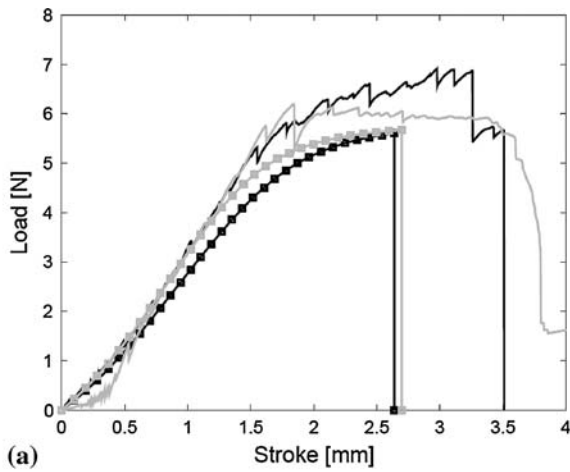


Fig. 7 The simulation of the hook deformation. It is assumed that the force direction remains perpendicular to the beam axis in the loading point



annealed at 350 - model annealed at 450 - exp.
 annealed at 350 - exp. annealed at 450 - model

Fig. 8 The graphs of the measured (*solid line*) and calculated (*square markers*) loading curves for samples S_{350_4.5} and S_{450_4.5} (a), S_{450_3.5} and S_{350_3.5} (b), and S_{350_2.5} and S_{450_2.5} (c)

that during bending the normal lines to the cross section areas ($\mathbf{n}_1, \mathbf{n}_2$ in Fig. 6) of the beam remain parallel to the beam axis. Furthermore, the superelasticity module of iRLOOP was used for each of the slices.

The boundary conditions are given by the fixation of the straight end of the hook (fixation of displacement and rotation)

Table 2 A comparison of the experimental and calculated maximum pulling forces

Sample	Maximum load—exp., N	Maximum load—model, N	Model inaccuracy, %
S_350_2.5	14.3	13.8	3.4
S_450_2.5	12.3	11.2	9.3
S_350_3.5	8.8	8.1	7.5
S_450_3.5	8.0	7.0	12.2
S_350_4.5	6.9	5.6	18.8
S_450_4.5	6.2	5.7	8.5

and by placing the loading force to the point, where the force direction is perpendicular to the beam axis (assuming thus a neglectable friction between hook and its counterpart, Fig. 7). By this way, we have obtained a movement of the loading point within the hook arc in our model similar to that observed in experiment. This loading point movement adds another non-linearity to the problem in addition to the material and geometrical ones.

Figure 8 shows the measured and calculated loading force versus stroke for all our samples listed in Table 1. The model input data for our simulation were the hook geometry and the tensile stress-strain curves in Fig. 5. There is a fairly good agreement between the calculated and the experimental curves at the beginning of the loading. Also, the prediction of the maximum pulling forces is close to the real respective values (Table 2). There is a certain disagreement in the maximum stroke of the measured and calculated curves. The reason for it is the simplification of the contact condition by neglecting any friction forces.

5. Hook Array, Manufacture, and the Measurement

In order to manufacture the hook arrays, two steel plates with the dimension $22 \times 22 \times 2 \text{ mm}^3$ and an array of microchannels with a diameter of 0.2 mm laser drilled in the plates were prepared. Two microchannel densities were realized: 121 and 441 holes per one plate evenly arranged in the area of 4 cm^2 . A rubber layer with a thickness of 2 mm was deposited on one side of either plate to allow individual inserted hooks to be fixed in each hole. After SMA hook insertion into the plate holes, a thin rubber layer was deposited at the other surface of the steel plate. This thin layer had a function to separate the steel plate from the resin that was deposited on the top of it. After resin curing at temperature $80 \text{ }^\circ\text{C}$ for 2 h, both the rubber layers and the steel plates were easily removed so that only the array of hooks connected together in the right positions by the cured resin remained. Finally, the straight hook ends on one side of the resin plate were polished away. In this way, the SMA hook array samples were ready for the mechanical experiments. The experimental setup is shown in Fig. 9.

Three series of mechanical tests were carried out. In each series, the interlocked SMA hook arrays were pulled apart along the axis that is perpendicular to both the array planes while force was measured until complete SMA hook release. In the first [third] series of experiments, we used the hook arrays with the low [high] densities (Fig. 10). In the second series, we used the hook arrays with low density on one side and the high density on the other side.

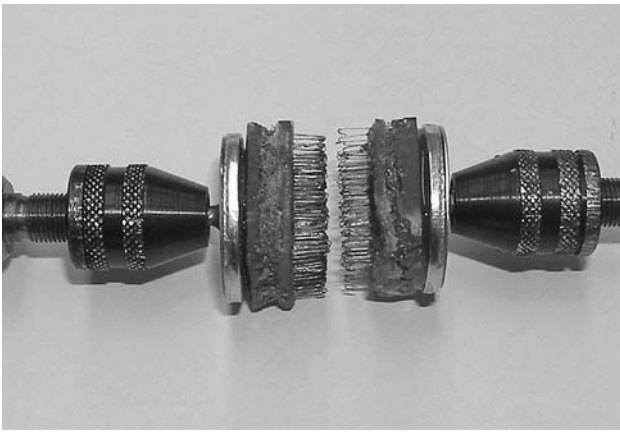


Fig. 9 Loading of SMA hook arrays

In Fig. 10, we show only the loading curves for the SMA hook arrays with the high density of SMA hooks. Since the number of the interlocked hooks is variable in each experiment and because at a given stroke each hook pair is in different stage of releasing, the loading curves in Fig. 10 are not overlapping and have a completely different character than those of Fig. 4. The maximum force lies inside a certain force interval in each series and the largest maximum force values are attained in the third series using SMA hook arrays with the high density. The mean values of the maximum forces in series 1, 2, and 3 are 5, 10, and 26 N, respectively. Hence, the maximum force may be optimized by changing SMA hook array density. Other force measurements such as measurements of the maximum force in shear loading and measurement of the maximum force during peel off are important for testing our superelastic applications. Therefore, in our further research, we plan to arrange the abovementioned measurements including the noise measurement during peeling off our SMA hook fasteners.

6. Conclusions

- (1) The minimum force necessary for the single SMA hook releasing strongly depends on the hook geometry and depends less on the hook heat treatment.
- (2) The model predicts the mechanic response well. The only disagreement in the maximum stroke before the unhooking event consists in the simplified contact condition. Based on the experimental and model data, the maximum force is increasing with the decreasing hook

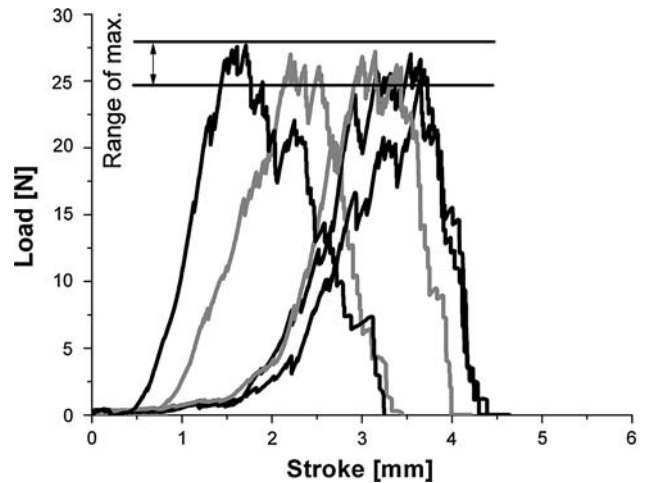


Fig. 10 The diagram of hook load vs. stroke for two SMA hook arrays with the high density of hooks. By the high density, we mean 441 hooks evenly arranged in the area of 4 cm^2

diameter. However for the diameters at the curved part of a hook $< 2.5 \text{ mm}$, plastic deformations develop after hook releasing (the wire diameter considered is 0.5 mm) and the hook does not return to its original shape any more.

- (3) A method for making SMA hook array was shown. This method enables us to form precise alignment of hooks and reach predefined hook densities.
- (4) The maximum force for normal direction loading of the SMA hook arrays may be optimized by changing the SMA hook array density.

Acknowledgments

D.V., D.M. and M.F. acknowledge support by a Marie Curie International Reintegration Grant within the 6th European Community Framework Programme. This research has also been supported by EC via FP6 integrated project AVALON (NMP2-CT-2005-515813). M.F. and P.S. acknowledge the Ministry of Education, Youth and Sports of the Czech Republic (MSMT) for financial support under Grant No. 1M06031.

References

1. Powell et al., U.S. Patent 7,032,282 B2
2. M. Frost, P. Sedlák, M. Sippola, and P. Šittner, *Smart Mater. Struct.*, in review
3. J.A. DeCastro, K.J. Melcher, R.D. Noebe, and D.J. Gazdosh, *Smart. Mater. Struct.*, 2007, **16**, p 2080–2090